



## POTASSIUM DETERMINATIONS USING SEM, FAAS AND XRF: SOME EXPERIMENTAL NOTES

Liritzis, I.<sup>1</sup>, Mavrikis, D.<sup>1,2</sup>, Zacharias, N.<sup>3</sup>, Sakalis, A.<sup>4</sup>,  
Tsirliganis, N.<sup>4</sup> and Polymeris, G.S.<sup>4,5</sup>

<sup>1</sup>*Lab. of Archaeometry, Dept of Mediterranean Studies, University of the Aegean,  
1 Demokratias Str., Rhodes 85100, Greece*

<sup>2</sup>*Lab. of Archaeometry, Institute of Materials Science, NCSR "Demokritos",  
15310 Aghia Paraskevi, Athens, Greece*

<sup>3</sup>*Lab. of Archaeometry, Dept. of History, Archaeology & Management of Cultural Resources,  
University of Peloponnese, 24100 Kalamata, Greece*

<sup>4</sup>*Lab. of Radiation Applications and Archaeological Dating, Department of Archaeometry  
and Physicochemical Measurements, Cultural and Educational Technology Institute, 'Athena' – Research  
and Innovation Center in Information, Communication and Knowledge Technologies,  
Tsimiski 58, GR-67100, Xanthi, Greece*

<sup>5</sup>*IŞIK University, Faculty of Science and Arts, Physics Department, TR-34980-Sile, Istanbul, Turkey*

Received: 15/09/2011

Accepted: 06/12/2011

Corresponding author: [liritzis@rhodes.aegean.gr](mailto:liritzis@rhodes.aegean.gr)

---

### ABSTRACT

The calibration of Scanning Electron Microscopy coupled with Energy Dispersive X- Rays Spectrometry (SEM-EDS) for elemental quantitative analysis is an important task for characterization, provenance and absolute dating purposes. In particular the potassium determination is an important contributor to dose rate assessments in luminescence and Electron Spin Resonance (ESR) dating. Here a SEM-EDX is calibrated on different archaeological and geoarchaeological materials against standard laboratory samples as well as measured by micro X-Rays Fluorescence ( $\mu$ XRF) and flame atomic absorption spectroscopy (FAAS) techniques. A common linear relationship is obtained for most elements and certain rock types used and two clear linear regressions for two types of rocks; one for granite, diorite, microgranite and sediments and another ceramic sherds, soils, marble schists, breccia. Such linear regressions become readily available for a future fast, efficient and accurate way of potassium determination.

---

**KEYWORDS:** calibration, potassium, SEM, XRF, rocks, ceramics, chemical elements

---

## INTRODUCTION

Archaeological materials (archaeo-materials i.e. artefacts, monuments) are identified and classified using scientific methods. These methods include physico-chemical analytical techniques which provide a 'chemical fingerprint'. The chemical fingerprints include characteristic (major, minor and trace) elemental composition of an archaeological artefact and allow determination of the provenance of material by comparison with the chemical fingerprint of an object of well documented (archaeologically, stylistically) origin. Such multi-analytical methods have become a powerful tool in the characterization and comparison of pottery and other rock types from an archaeological context. Of these elemental abundances K, U, Th and Rb are also useful for luminescence and ESR dating purposes as prerequisite parameters in dose-rate determination (Aitken, 1985; Liritzis et al., 2010a).

Analytical techniques and data have been published and a large amount of data on the chemical composition of pottery has been produced over the past few decades (e.g. Jones, 1986; Pollard & Heron, 1996).

Theoretically this database, allows the clustering and identification of newer finds of ceramic artefacts. However, experience has shown the importance of calibration of the employed instrumentation for the material type analysed. For example, archaeomaterials exhibit differences due to matrix effects that includes grain size and composition, density, porosity, effective atomic number, homogeneity, humidity. The impact of all these on calibration is enhanced with the different physical principles of operation of the various applied techniques (e.g. X-Ray Florescence (XRF), Flame Atomic Absorption Spectroscopy (FAAS), Scanning Electron Microscope (SEM) coupled with energy dispersive spectroscopy (EDS), Inductively Coupled Plasma (ICP), Neutron Activation analysis (NAA), Laser Induced Breakdown Spectroscopy (LIBS), Optical Emission Spectroscopy (OES), to mention a few but major ones) (Janssens & Van Grieken, editors, 2004)

Here we present a case study for calibrating a SEM-EDS with various types of materials

measured by FAAS,  $\mu$ XRF and standard materials (Table 1) with emphasis on potassium (K) determination, a useful element for the dating by TL or OSL luminescence techniques. The radioactive isotope  $^{40}\text{K}$  emits  $\beta$ - and  $\gamma$ -rays that contribute a great amount in the total dose-rate of materials (external and internal radiation) dated by luminescence (Aitken, 1985). In particular, the  $^{40}\text{K}$  contribution is a major issue often encountered in fieldwork or museum cases of, a) low environmental gamma ray dose rate (e.g. a calcareous material or calcareous fortified walls, in surface dating of exposed materials), b) feldspathic rocks (e.g. in granites, basalts, gneiss), c) granites, with apparent mineral inhomogeneity, d) samples with built up of surrounded sedimentary layers made by diversified (non homogeneous) nature of chemical/petrological composition (e.g. tsunami deposits, cave deposits, sea sediments, whereas K may vary a great deal with more impact on dose rate than U, Th variation), e) authenticity testing of museum objects where often no environmental radiation is known and sample's K is usually a major dose rate emitter. An illustrative discussion on the contribution of K to the total dose and consequently to the age estimation of archaeological pottery following fine- and coarse-grain luminescence dating can be found at Zacharias et al. (2005).

In addition, the microdosimetry in dating single aliquots of grains depends on the U, Th, K, Rb distribution around the aliquot. Although, the single aliquots average out such non-smoothed mineral distributions as they are collected from a larger than their size area/volume of the sample, the possibility to get a wide range of doses (and outliers), in particular on rock surface dating and sun-bleached sediments, is possible. This is more pronounced in single grain aliquots. In any case, the exact determination of potassium values (as  $\text{K}_2\text{O}\%$  or  $\text{K}\%$ ) is a major need and rapid and accurate measurement are desirable. We present here a simple way to determine potassium values with a high precision employing the SEM facility at the Institute of Materials Science, National Centre for Scientific Research "Demokritos" (Athens). This was calibrated on samples with different composition that were measured with

other well calibrated techniques such as, flame atomic absorption spectroscopy (FAAS),  $\mu$ -XRF (were performed at Laboratory of Radiation Applications and Archaeological Dating, Department of Archaeometry and Physicochemical Measurements, CETI, Xanthi) using well

calibrated Standards (see Table 1). In addition to K% some other oxides of elements with atomic numbers ranging from 11-26 are presented, and for these appropriate calibration are devised which can be used for future analytical projects.

**TABLE 1: Samples, type of materials, manufacturer and references**

Sample	Type	Provenance/Reference	Technique
G94	Threlkeld microgranite	GIT-IWG (Thompson et al., 1996)	Standard (XRF, ICP – AES, INAA, AAS, wet chemistry) K <sub>2</sub> O=2.91±0.09% SiO <sub>2</sub> =69.95±0.57% MgO=1.036±0.015% CaO=1.34±0.02% Na <sub>2</sub> O=4.54±0.03% TiO <sub>2</sub> =0.306±0.011% Fe <sub>2</sub> O <sub>3</sub> =3.04±0.13% Al <sub>2</sub> O <sub>3</sub> =14.53±0.19%
OU1	Fine-grained grey-green volcanic tuff partially recrystallized.	GeoPT2 Thompson et al., 1998	(XRF, ICP – AES, INAA, AAS, wet chemistry) K <sub>2</sub> O=0.215±0.002% SiO <sub>2</sub> =58.03±0.58% MgO=4.69±0.14% CaO=6.23±0.44% Na <sub>2</sub> O=2.49±0.16% TiO <sub>2</sub> =0.46±0.02% Fe <sub>2</sub> O <sub>3</sub> =9.25±0.52% Al <sub>2</sub> O <sub>3</sub> =14.98±0.42%
OU2	Belford dolerite	GeoPT4 (Thompson et al., 2000)	Standard (XRF, ICP – AES, INAA, AAS, wet chemistry) K <sub>2</sub> O=0.95±0.09% SiO <sub>2</sub> =51.1±0.6% MgO=5.72±0.14% CaO=8.24±0.20% Na <sub>2</sub> O=2.42±0.06% TiO <sub>2</sub> =2.32±0.15% Fe <sub>2</sub> O <sub>3</sub> =13.11±0.11% Al <sub>2</sub> O <sub>3</sub> =14.26±0.42%
OU3	Nanhoron microgranite	GeoPT6. (Thompson et al., 2000)	Standard (XRF, ICP – AES, INAA, AAS, wet chemistry) K <sub>2</sub> O=4.581±0.17% SiO <sub>2</sub> =74.46±0.20% MgO=0.017±0.006% CaO=0.204±0.003% Na <sub>2</sub> O=3,721±0.017% TiO <sub>2</sub> =0.224±0.003% Fe <sub>2</sub> O <sub>3</sub> =3.812±0.012% Al <sub>2</sub> O <sub>3</sub> =12.99±0.03%
JG2	Granite	GSJ (Potts et al., 1992; Korotev, 1996)	Standard (XRF, ICP – AES, INAA, AAS, wet chemistry) K <sub>2</sub> O=4.72±0.20% SiO <sub>2</sub> =76.95±0.20% MgO=0.04±0.0007% CaO=0.80±0.015% Na <sub>2</sub> O=3.55±0.018%

			TiO <sub>2</sub> =0.04±0.006% Fe <sub>2</sub> O <sub>3</sub> =0.36±0.004% Al <sub>2</sub> O <sub>3</sub> =12.41±0.05%
JG3	Granodiorite	GSJ (Potts et al., 1992; Korotev, 1996)	Standard (XRF, ICP – AES, INAA, AAS, wet chemistry) K <sub>2</sub> O=2.63±0.1% SiO <sub>2</sub> =67.10±0.30% MgO=1.79±0.02% CaO=3.76±0.05% Na <sub>2</sub> O=4.03±0.03% TiO <sub>2</sub> =0.48±0.007% Fe <sub>2</sub> O <sub>3</sub> =1.61±0.09% Al <sub>2</sub> O <sub>3</sub> =15.52±0.08%
AC-E	Microgranite	GIT-IWG (Potts et al., 1992; Korotev, 1996)	Standard (XRF, ICP – AES, INAA, AAS, wet chemistry) K <sub>2</sub> O=4.49±0.02% SiO <sub>2</sub> =70.35±0.07% MgO=0.03±0.01% CaO=0.34±0.02% Na <sub>2</sub> O=6.54±0.04% Fe <sub>2</sub> O <sub>3</sub> =1.34±0.06% Al <sub>2</sub> O <sub>3</sub> =14.7±0.05%
RHO-877	Brecciated Sediment	From the archaeological excavation site at Cheiming-Stottham (Liritzis et al., 2010b)	FAAS K <sub>2</sub> O=2.31± 0.1%
RHO-1015	Soil	Chieming-Stottham: Soil from impact layer (Liritzis et al., 2010b)	FAAS K <sub>2</sub> O=1.78± 0.08%
RHO-886	Fractured cobbles	Chieming-Stotthan impact layer: shock effects? (Liritzis et al 2010b)	FAAS K <sub>2</sub> O=0.001± 0.0001%
KAPS4	Marble schist	Styra region Liritzis et al., 2010a	FAAS K <sub>2</sub> O=0.089± 0.04%
1/LP4	Marble schist	Styra region Liritzis et al., 2010a	FAAS K <sub>2</sub> O=0.313±0.015%
3/LP3A	Marble schist	Styra region Liritzis et al., 2010a	FAAS K <sub>2</sub> O=0.36±0.015%
P1	Schist	Styra region Liritzis et al., 2010a	FAAS K <sub>2</sub> O=0.577±0.026%
P2	Schist	Styra region Liritzis et al., 2010a	FAAS K <sub>2</sub> O=0.479±0.022%
Bonn Ceramic standard	Ceramic	University Bonn Archaeological Science Group, Institut für Stahlen- und Kernphysik, University Bonn, Nussallee 14-16, D-53113 Bonn	NAA, XRF K <sub>2</sub> O=1.33±0.39%
5-3 M3 soil	Soil	Chieming- Stottham excavated section, Germany (Liritzis et al., 2010b)	μXRF K <sub>2</sub> O=0.96±0.10%
5-3 M4	Soil	Chieming-Stottham Excavated section, Germany (Liritzis et al., 2010b)	μXRF K <sub>2</sub> O=1.113±0.042%
5-3 M4 (surrounded soil)	Soil	Chieming- Stottham excavated section, Germany (Liritzis et al., 2010b)	μXRF K <sub>2</sub> O=0.770±0.014%

5-4 M Br	Brecciated sediment	Chieming- Stottham, Germany (Liritzis et al., 2010b)	$\mu$ XRF K <sub>2</sub> O= 0.857±0.015%
5-2 fBv	Loam	Chieming- Stottham, Germany (Liritzis et al., 2010b)	$\mu$ XRF K <sub>2</sub> O=1.417±0.084%
RHO-878	Soil	Marwang, Germany (Liritzis et al., 2010b)	$\mu$ XRF K <sub>2</sub> O=0.920±0.060%
5-3 M5	Soil	Chieming-Stottham, Germany (Liritzis et al., 2010b)	FAAS 1.755±0.08%
Nos. 16, 23, 34, 35	Ancient ceramic sherds	c/o CETI, Xanthi	FAAS 16) K <sub>2</sub> O=1.203±0.06% 23) K <sub>2</sub> O=1.936±0.08% 34) K <sub>2</sub> O=1.427±0.07% 35) K <sub>2</sub> O=1.278±0.06%

## 2. INSTRUMENTATION & SAMPLES

### SEM-EDX

Energy-dispersive X-ray spectroscopy (EDS or EDX) is an analytical technique used for the elemental analysis or chemical characterization of a sample. It is one of the variants of X-ray fluorescence spectroscopy which relies on the investigation of a sample through interactions between electromagnetic radiation and matter, analyzing the X-rays emitted by the matter in response to being hit with charged particles. The difference with  $\mu$ XRF is the different exciting agents; electrons in SEM and primary X-Rays in XRF. Scanning Electron Microscopy (SEM) coupled with energy dispersive X ray spectrometry (EDX) analysis (Philips FEI-Quanta INSPECT with SUTW (super ultra-thin window) detector and coupled with EDS PV7760) was used. Quantitative analysis used software EDS-Genesis with errors computed via ZAF correction. ZAF - for atomic number Z, Absorption A and Fluorescence for F - uses fundamental factors to correct for the effects of atomic number, absorption and fluorescence. Analyses were performed at 25 keV with 35° take-off angle. More reliable analyses are these for elements contained in concentrations >0.1%. An error of around 5 to 10% is accounted, for the major elements. Samples for SEM were grounded down to powder with grain size 50 - 100  $\mu$ m pressed (90-120 bars) to a cylindrical shape (pellets) of size 8 mm diameter and 1 mm thickness, carbonized and measured.

### AAS

In AAS measurements the flame atomization mode was selected for K determination, a Perkin Elmer (USA) instrumentation, model Analyst 800 atomic absorption spectrophotometer was used. The dissolution of the samples was achieved using a model CEM (USA) model MARS5 microwave digestion oven. Typically, a few grams of sample was grounded using an agate mortar and dried for 2h at 102°C in laboratory furnace (Lindberg/Blue, model BF 51866C, USA). Of this, 0.25gr of each sample were accurately weighted and mixed with 6.3ml 48% HF (Panreac) and 6.3ml HNO<sub>3</sub> 65% (Merck) in suitable teflon vessels and optimized pressure/temperature program in the microwave oven was run with following settings.

Max Voltage (W)	Power (%)	Ramp time (min)	Pressure (psi)	Temperature (°C)	Hold time (min)
600	85	30	150	210	15

After the dissolution the samples were diluted to a final volume of 100ml and analyzed using FAAS. The reagents used were of analytical grade of purity. A standard reference solution (1000 ppm K) was used for the construction of the calibration curves was purchased from Perkin Elmer (USA).

### $\mu$ -XRF

A few grams of each sample was carefully grounded and dried for 2h at 102°C in laborato-

ry furnace. After drying, 5.00gm of each sample was thoroughly mixed with a binder (cellulose) using a ratio 4:1 (1.25gm of binder). Finally the mixture sample/binder was pressed in a 32mm mould under a pressure of 12t using a manual hydraulic press (Specac, UK), creating the sample tablets ready for analysis. The standard reference material SARM69 (MIIntek, Republic of South Africa). Was used for the quantification of the results. A state-of-the-art compact micro X-Ray Fluorescence spectrometer was used for the XRF measurements.

This instrument comprises a side-window X-ray tube with Mo anode (Series 5011 XTF, Oxford Instruments) with maximum voltage and current of 50 kV and 1 mA respectively, together with a solid state Si(Li) Peltier-cooled X-Ray detector (8  $\mu\text{m}$  Be window, 3.5 mm<sup>2</sup> active area, 300  $\mu\text{m}$  nominal thickness and resolution 149–166 eV at the Mn K<sub>a</sub> energy).

A long distance optical microscope was used to locate the focal spot on the sample surface. The nominal beam diameter is <150  $\mu\text{m}$  at the position of the sample and the X-ray optics include a straight monocapillary lens. The samples were placed on a rotating holder mounted on a motorized XYZ stage (NewPort PRL-12 with 0.1 mm step size, travel distance of 5 cm in the X-, Y-direction and 2.5 cm in the Z-direction). Geometry of 48°/42° (excitation / detection) was used while the relative angle between the X-ray tube and the detector is fixed at 90°.

The operating conditions during the micro-XRF measurements were 35kV applied potential, 0.9mA current and 5min spectrum acquisition in real time. Three micro-XRF measurements were performed in a non-destructive way in a point scan mode on several points on the sample tablet. For spectra interpretation and data quantification, a customized software (WinAxil, Canberra, BENELUX) was used. This instrument has the advantage of point analysis on the surface though other portable XRF may detect an area of 25 mm on the surface which is more representative.

This is however at the expense of the side effects of the aperture. The latter has been investigated by one of us (IL) to measure K and other elements devising experimental design for dependence of accuracy on grain size, sample

thickness and Z<sup>1</sup> (Liritzis, 2007; Liritzis and Zacharias, 2011). These authors have found that the dependence of K concentration as a function of percentage coverage of PXRF aperture for four positions for the Spectrace 9000 TN is considerable. Thus, for 100% to about 25% coverage elemental K concentration varies by a about x9 fold factor. At any rate, sample mineralogy (grain size and grain distribution), but also the percentage covering of analyzer window with solid flat artifacts, as well as, correction factors has to be taken into account in window types XRF detectors as shown in Liritzis and Zacharias (2011).

The samples are given in Table 1. Standard samples with nominal values are taken from Potts et al., 1992 and references therein.

### 3. MEASUREMENTS

Three measurements for respective element oxides were taken for each sample by SEM and their average along with the standard deviation is plotted in bi-plots against the known values from the other techniques. Two linear covariances are apparent and those and some dispersions are discussed below. They were measured for K and oxides of Na, Mg, Al, Si, Ca, Ti, Fe.

For potassium (K) (Fig. 1), two distinct linear curves, corresponding to two group of samples with both having a satisfactory statistical R-squared significance, the following can be seen: Group A consists of samples that include marble schists (from archaeological monuments), the majority of the sediments, soil samples and ceramics; Group B consists of granitic samples, diorites, a Bonn ceramic standard and a few sediments. The formation of two trends should be attributed to two reasons: the highly calcitic nature of Group A samples in contrast to Group B samples and the longer range of values for Group B in relation to Group A. Both groups were measured for K, while the other element oxides were available from only the one group. The following plots were obtained: For *Calcium*

---

<sup>1</sup> Initial readings for this were taken by assistants in the Lab. of Archaeometry, Rhodes, under supervision, experimental design and interpretation of IL and then after 2 years in 2007 by IL and technician Dr A. Vafiadou.

(Fig. 2a) a linear fit is apparent for all standards. For *Iron* (Fig. 2b) a similar to Ca linear fit is obtained which within the errors and the number of samples care a ratio 1:1.

For *Magnesium* (Fig. 2c) the linear fit is disturbed for OU1 and CAL-S (pure CaCO<sub>3</sub> 39.64 % calcite). For *Silicon* (Fig. 2d-1, d-2) a linear fit with a little dispersion is obtained the data shown in two scales, for *Aluminium* (Fig. 2e) a linear fit for all with little dispersion, for *Sodium* (Fig. 2f) a linear fit with some dispersion for AC-E and Bonn, and for the *Titanium* (Fig. 2g) a linear fit is obtained with large error bars for OU2 and the Bonn ceramic clay.

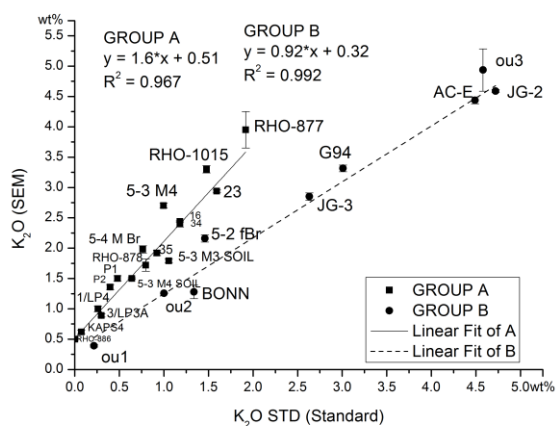


**Fig. 1 Potassium. K<sub>2</sub>O by SEM versus K<sub>2</sub>O by other techniques. Standard in abscissa refer to the measured elements by FAAS and μXRF and by the quoted reference sources. Error bars shown, in other cases are within the point symbol (see, Table 1).**

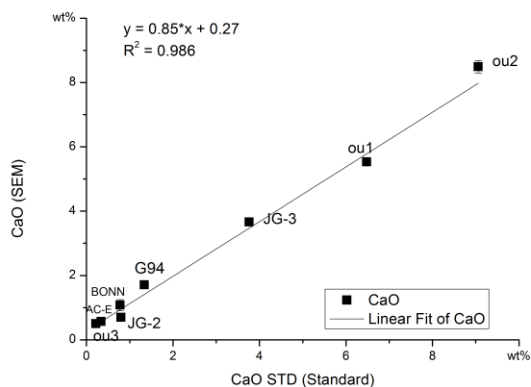


**Fig. 2a Calcium Oxide**

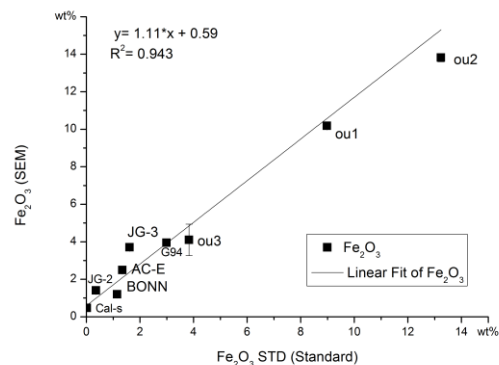


**Fig. 2b Iron Oxide**

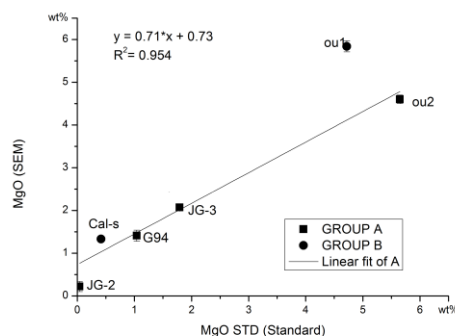


**Fig. 2c Magnesium Oxide**

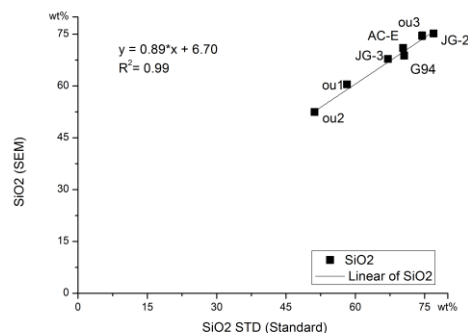


**Fig. 2d-1 Silicon Oxide**

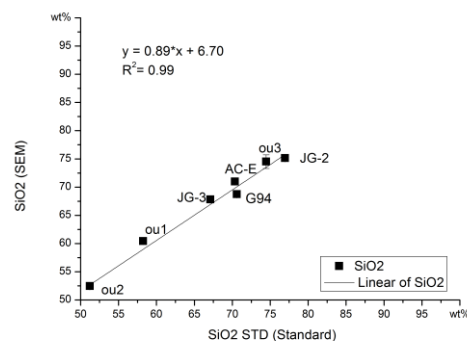


**Fig. 2d-2 Silicon Oxide**

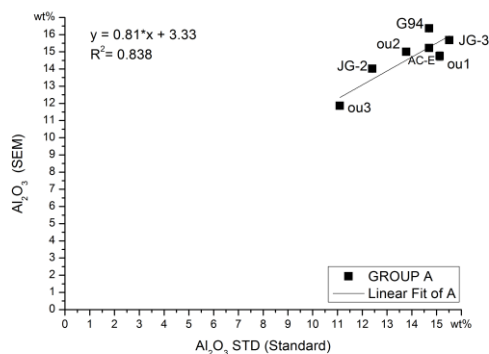


Fig. 2e Aluminium Oxide

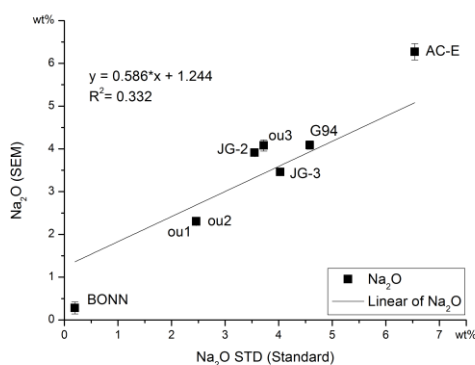


Fig. 2f Sodium Oxide

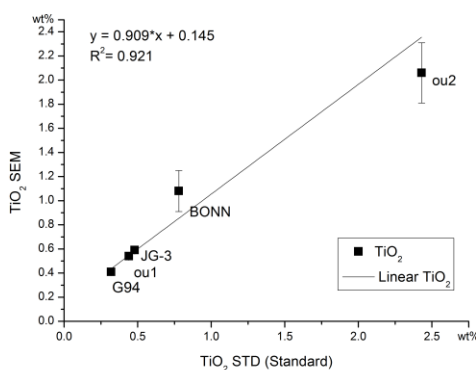


Fig. 2g Titanium Oxide

#### 4. DISCUSSION & CONCLUSION

The use of SEM-EDX for elemental analysis on a provided standard material, usually accompanying the equipment, is not a safe guide. Some of the standards chosen for routine electron microprobe analysis are not optimal for routine analyses of different types of rocks (e.g. silicates, metals, oxides). Metal standards will need large dead-time and atomic number corrections that would be minimized with oxide or silicate standards.

The importance of using standards with similar compositions to unknowns to minimize the still approximate ZAF corrections is vital. For example, the use of pyrite as a standard for S in analysis of sulfates or sulfate-bearing silicates will produce large systematic errors caused by significant characteristic wavelength shifts due to bonding differences between sulfides and sulfates (Goldstein et al., 2003).

A more specific calibration should be made. Here, for a wide spectrum of materials type we have shown that the calibration of SEM provides a linear fit for  $K_2O$ ,  $SiO_2$ ,  $TiO_2$ ,  $Fe_2O_3$ ,  $Na_2O$ ,  $Al_2O_3$ ,  $MgO$  and  $CaO$ . (Potts, 1987)

The granites and diorites and some sediments follow a different calibration curve in comparison with other types of materials (soils, ceramic, schists, marble schists). At a first glance it is observed that volcanic origin materials have a different behavior, that implies mineralogy plays a major role in SEM counting techniques for elemental composition. Here the effective-Z of measured materials, as well as, other phenomena affect X-ray escape and recording, as discussed below to explain the different linear curve for the analyzed material types. Indeed, the accuracy of an X-Ray EDS spectrum is determined by many factors such as detector windows that may absorb low-energy X-rays; over-voltage settings that may shift (observed two sided expansion) the spectrum to the larger energies making higher-energy peaks larger and lower-energy peaks smaller; overlapping peaks; the nature of the sample - produced X-rays may not all escape the sample and this in turn depends on the energy of the X-ray and the amount and density of material it has to pass through. These, can result in reduced accuracy in inhomogeneous and rough samples.

In SEM-EDS the ZAF factors are a function of composition of samples. The quality of analyses performed depends on the quality of sample preparation, character of the sample material, and availability of appropriate primary and secondary calibration standards for the desired elements. The atomic number effect controls the amount of incident energy from the electron beam that is actually put into the sample. This effect consists of two components: backscattering and electron-stopping power (or retarda-

tion). Both are a function of average  $Z$  and, to a lesser degree, the accelerating voltage.

Backscattered electrons leave the sample carrying energy without producing X-rays. The fraction of electrons backscattered from the sample,  $n_b$ , ranges from about 0.12 for Al to 0.55 for U. At lower  $Z$ , more electrons stay within the sample to produce X-rays. The backscatter correction factor,  $F_b$ , reflects the X-ray intensity lost due to backscattering and is expressed as a fraction ( $r$ ) relative to the intensity that would be produced with no backscattering.

Calibration curves constructed here relate X-ray counts and element concentration. However, such curves require a large number of well-characterized standards with compositions that bracket the unknowns. In wet chemical analysis, such as atomic absorption spectroscopy (AAS), it is relatively easy to make solutions with the appropriate concentrations.

In contrast, production of standards for microprobe analysis is far more difficult, requiring apparatus to produce homogeneous glasses. In both cases, however, the data used to construct a curve must be taken at identical operating conditions (take-off angle, accelerating voltage and beam current) as will be used during analysis. For geological applications and geoarchaeological materials, calibration curves must be constructed for each mineral group. In cases that the unknowns approximate the standards in compositions, matrix corrections are unnecessary. The requirement of a great number of standards is especially difficult to satisfy especially with the accuracy required. In addition, this technique does not allow confident analysis of a truly unknown material. That is why we investigated the calibration with a variety of archaeological and geoarchaeological materials.

In X-rays from SEM, however, matrix effects due to absorption and fluorescence of X-rays within the sample and atomic number effects are significant. ZAF is not very good for elements with X-ray energies less than 1 keV because of a lack of knowledge of the factors discussed below. For these elements it is best to use a standard of similar composition to minimize matrix effects.

The atomic number effect controls the amount of incident energy from the electron beam that is

actually put into the sample. This effect consists of two components: backscattering and electron-stopping power (or retardation). Both are a function of average  $Z$  and, to a lesser degree, the accelerating voltage (see [http://www.microbeamanalysis.org/topical-conferences/particles-2009/PTC2009\\_Armstrong.pdf](http://www.microbeamanalysis.org/topical-conferences/particles-2009/PTC2009_Armstrong.pdf))

Since X-rays (in SEM or for the  $\mu$ XRF) are generated below the surface of the sample, the emergent radiation suffers absorption prior to detection. The absorption correction is a function of the take-off angle (length of path traversed by the X-rays), the distribution of X-ray generation, the wavelength of the emergent X-ray and the elements present. As the take-off angle increases, the intensity of characteristic radiation decreases due to an increase in path length. Less energetic X-rays are more easily absorbed. Absorption can also be strongly affected by surface irregularities -- a good sample polish is thus critical. Most X-rays are generated at relatively shallow depths within the excitation volume and relatively close to the beam axis, because it is in this region that electron energies are greatly attenuated by ionization or electron scattering. Several models have been used to describe the depth distribution of X-ray generation.

The fluorescent yield increases rapidly with increasing atomic number and fluorescence factor  $F_f$  is negligible for K-lines of elements below atomic number 20. In silicates and oxides, absorption dominates and fluorescent enhancement is rarely greater than a few percent. Thus, the  $Z$  effects (backscattering factor, retardation of the electrons, and effective ionization cross-section) are a matter of proper modeling correction and other correction models may produce a better determination especially of the absorption effects.

Occasionally  $\mu$ XRF also did not provide values comparable to the apparent linear fit with SEM or FAAS, This was due to small area that was analyzed, by the focused X ray beam, and partly to the single standard used for the quantification of all different material types. It is thus, recommended that in such cases, several points on the sample surface be analyzed to get average values. FAAS values are more representative as the method averages out the oxide distribution due to the complete dissolution

and flame atomization. In cases of homogeneous samples (e.g. loam, thin soil layer etc.) the measurement is more representative.

The obtained bi-plots are useful calibration curves for measuring accurately potassium (and some other oxides) values, which are important

in dating of materials particularly by employing the luminescence techniques (TL, OSL) where multi-elemental/multi-phase natural materials (e.g. breccias of tectonic genesis) or even man-made composite means (e.g. plasters) are subject to absolute dating.

## ACKNOWLEDGEMENTS

We thank Prof. Marco Martini (Italy) and Prof. Ashok Singhvi (India) for constructive comments and Dr Y.Bassiakos for useful comments. DM thanks directorate of NCPR "Demokritos" for permission to use their premises.

## REFERENCES

- Aitken, M. J. (1985). *Thermoluminescence dating*. Academic Press, London.
- Goldstein, J, Newbury, D.E, Joy, D.C, Lyman, C.E, Echlin, P, Lifshin, E, Sawyer, L, and Michael, J.R (2003) *Scanning Electron Microscopy and X-Ray Microanalysis*. Springer; 3rd edition.
- Gills, T. E. (1993). *Certificate of Analysis, Standard Reference Material 2711*, National Institute of Standards and Technology, Gaithersburg
- Janssens, K and Van Grieken R (eds) (2004) *Non destructive microanalysis of cultural heritage materials*. Vol.XLII, Wilson & Wilson's Comprehensive Analytical Chemistry, Volume Series edited by D.Barcelo, Elsevier.
- Jones, R., (1986) *Greek and Cypriot Pottery: A Review of Scientific Studies*. In: Fitch Laboratory Occasional Paper, vol. 1. British School at Athens.
- Korotev, R.L. (1996). Self-Consistent Compilation of Elemental Concentration Data for 93 Geochemical Reference Samples. *Geostandards Newsletter*, 20, 217-245.
- Liritzis, I, Polymeris, S.G and Zacharias, N.(2010a) Surface luminescence dating of 'Dragon Houses' and armena gate at Styra (Euboea, Greece). *Mediterranean Archaeology & Archaeometry*, Vol.10, No.3, 65-81
- Liritzis, I., Zacharias, N., Polymeris, G.S., Kitis, G., Ernstson, K., Sudhaus, D., Neumair, A., Mayer, W., Rappenglück, M.A., Rappenglück, B. (2010b) The Chiemgau meteorite Impact and tsunami event (southeast Germany): First OSL dating. *Mediterranean Archaeology & Archaeometry*, Vol.10, No.4, 17-33.
- Liritzis, I and Zacharias, N (2011) Portable XRF of Archaeological Artifacts: Current Research, Potentials and Limitations. In M.S. Shackley (ed.), *X-Ray Fluorescence Spectrometry (XRF) in Geoarchaeology*, Chapter 6, Springer Science, 109-142.
- Potts P.J., Tindle, A.G, Webb, P.C. (1992). *Geochemical Reference Material Compositions: Rocks, Minerals, Sediments, Soils, Carbonates, Refractories & Ores Used In Research & Industry*, Boca Raton : CRC Press
- Potts, P.J., (1987) *A Handbook of silicate rock analysis*. Blackie, Glasgow and London.
- Pollard, A.M.and Heron, C., (1996) *Archaeological Chemistry*. The Royal Society of Chemistry, London, UK.
- Thompson, M., Potts, P.J., and Webb, P.C. (1996). GeoPT1. International proficiency test for analytical geochemistry laboratories - Report on round 1 (July 1996). *Geostandards Newsletter*, 20, 2, 277-287.
- Thompson, M., Potts, P.J., Kane, J.S., Webb, P.C., and Watson, J.S. (2000). GeoPT4. An international proficiency test for analytical geochemistry laboratories - report on round 4 (March 1999). *Geostandards Newsletter: The Journal of Geostandards and Geoanalysis*, 24, 1, 135.

- Thompson M., Potts P.J., Kane J.S., Webb P.C. and Watson, J.S (1998). GeoPT2. International proficiency test for analytical geochemistry laboratories. Report on round 2. *Geostandards Newsletter: The Journal of Geostandards and Geoanalysis*, 22: 127-156.
- Tite M.S. and Waine J. (1962). Thermoluminescence dating: a re-appraisal. *Archaeometry*, 5, 53-79.
- Zacharias, N., Buxeda i Garrigos, J., Mommsen, H., Schwedt, A., Kilikoglou, V. (2005). Implications of burial alterations on luminescence dating of archaeological ceramics, *J. Archaeological Science*, 32.1, 49-57.